Point Viscosity Measurements in a Fluidized Bed

WILLIAM W. SHUSTER and FREDERICK C. HAAS
Rensselaer Polytechnic Institute, Troy, N. Y.

A NUMBER of investigators have proposed that a modified Stormer viscometer be used to measure the simulated viscosity of a fluidized bed (*1, 4*). While this method of measurement does not produce a true viscosity measurement because of the particle accelerations and added interparticle frictional effects which occur in conjunction with the normal shearing stress, it has been shown to be related to the flow characteristics of a bed. Throughout this paper the terms, "simulated viscosity" and "viscosity" are used interchangeably to mean the viscosity of a fluidized bed as measured by such a device.

Matheson, Herbst, and Holt (*4*), the first investigators to assign viscosity values to fluidized beds, observed that simulated viscosity was very useful in predicting the flow properties of a fluidized bed. Because their work was done in a small column with a paddle which was appreciable in size compared to the column diameter, they ascribed but one value of viscosity to a bed.

Kramers (*3*) measured vertical viscosity profiles in a fluidized bed by means of a rotating dumbbell. His experiments showed that the resistance of a body dragged through a fluidized bed is very sensitive to structural changes in the bed and that viscosity changes as a direct function of the turbulence in a bed.

Furukawa and Ohmae (*1*), in an extensive study to correlate the properties of a fluidized bed to the properties of ordinary liquids, postulated that the equivalent variable of liquid temperature was the product of the fluid viscosity and velocity. Their viscosity work covered a large range of bed expansions and they found the viscosity of a binary system of coarse and fine particles generally obeyed Kendahl's relation for liquids:

$$\text{Log } \mu_{mix} = y_a \log \mu_a + y_b \log \mu_b$$

This investigation studied the simulated viscosity of a fluidized bed at various points in a relatively large column as a function of various operating variables. The effects of longitudinal paddle position, radial paddle position, particle size distribution, and the type of fluid distributor were studied in beds of glass beads fluidized by air.

THEORY

The Stormer viscosity is measured by observing the weight required to rotate a paddle immersed in a fluid at a constant angular velocity. Such a weight may, therefore, be visualized as the force necessary to overcome the resistance of the fluid to flow.

On a microscopic scale, a single particle striking the paddle, rotating at a constant speed, will have its velocity vector changed in both speed and direction unless the collision is entirely elastic. If it is assumed that the initial velocity vector is in the vertical direction, the collision between the particle and the paddle will occur on the forward paddle face (the face cutting the medium) rather than the back face, because the paddle is continually turning into the path of the particle, applying a shearing action to the path of the particle. The impact between the paddle and particle causes a resistance to rotation and, in order to maintain a constant angular paddle velocity, this resistance must be compensated for by an additional weight applied to the paddle. Because a particle having a horizontal component of velocity may strike either the front or back face of the paddle, the effects of such collisions tend to cancel out. On a macroscopic scale, the measured viscosity is a summation of the impact resistances, which in turn constitutes a measure of the number of particles striking the paddle. The viscosity is thus a direct indication of the uniformity and degree of turbulence in the bed.

The viscosity of a fluidized bed as measured by a Stormer viscometer is a function of paddle size, paddle angular velocity, particle size, particle density, particle size distribution, bed density, and fluid velocity. For a given fluid bed and viscometer, it is of interest to postulate the effects of fluid velocity and bed density on the simulated viscosity, other variables being held constant.

As the simulated viscosity is dependent on the number of collisions between the viscometer paddle and the bed particles, viscosity would be expected to be a direct function of the bed density (number of particles per unit bed volume).

As the fluid velocity through a bed is increased, the kinetic energy of the individual particles is increased, in general, because of increased particle velocity. The increased particle velocity causes more particles to pass into the region of the paddle path per unit of time. Since the viscosity is an average measurement taken over a period of time, an increased number of particles strike the paddle at constant bed density. Thus, at constant bed density, the viscosity would be expected to increase with an increase in fluid velocity.

Because bed density is to a certain extent a function of fluid velocity, it is of interest to consider how viscosity might be expected to vary with fluid velocity, beginning with a fixed bed just before it starts its initial bed expansion. A hypothetical variation in viscosity with fluid velocity is shown in Figure 1, with three separate regions indicated.

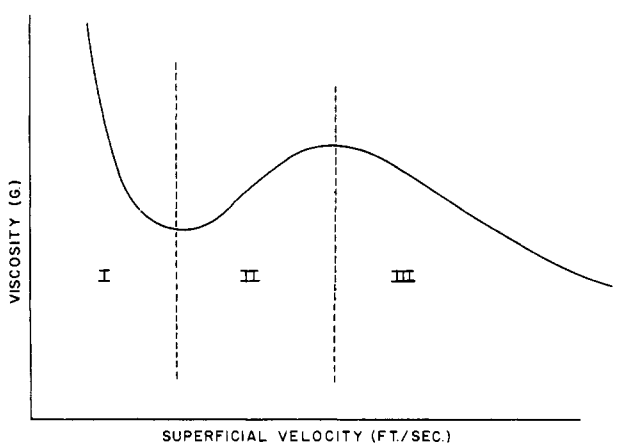

Figure 1. Theoretical variation of viscosity with flow rate

In Region I the viscosity decreases very rapidly with small increases in fluid velocity, because of aeration of the bed which causes the static particle inertia forces to disappear quickly and the bed density to decrease. Little particle movement is observed in this region. In Region II particle motion increases with increased fluid velocity as the particles tend to redistribute themselves with little change in bed density (5). As a consequence, the increased number of collisions with the paddle becomes the controlling factor and results in a net increase in viscosity. In Region III, increased fluid velocities cause the bed density to decrease and once more to become the controlling factor affecting viscosity, until at very high velocities an equilibrium is approached between the bed density effect and the particle velocity effect.

MATERIALS AND APPARATUS

The fluidized beds were contained in a Lucite column having an inside diameter of 5.75 inches. The beds were supported on one of the two gas distributors studied in this work: a 200-mesh stainless steel screen supported on a coarser screen, and a $\frac{1}{8}$-inch, class B, Micro Metallic stainless steel porous plate. Air was supplied to the column by a Roots-Connersville blower and its rate measured by calibrated Flowraters. Provisions were made for temperature and pressure measurements. The apparatus is shown in Figure 2.

The instrument used for measuring the simulated viscosity of a fluidized bed was a commercial Stormer viscometer modified for use in this study. A paddle having dimensions of $\frac{3}{4} \times \frac{3}{4} \times \frac{1}{16}$ inch was mounted on an extended shaft, replacing the standard unit. The viscometer was removed from its base and mounted on a special positioner which allowed placement of the paddle at any desired horizontal or vertical point in the bed.

Glass beads, being spherical in shape and giving beds of high viscosity, were chosen as the fluidized material. Their dimensions are given in Table I. Beads 4 through 13 were used for single-size studies, while beads 090 through 150 were used in mixture studies.

EXPERIMENTAL PROCEDURE

To determine the viscosity of a particular quantity of a given size or size distribution of beads, the viscometer paddle was located at the desired position in the bed. The air flow was established at a chosen rate, and the weight necessary to rotate the paddle at a standard speed was determined. The weight required to rotate the paddle at the same speed and with the same air velocity in an empty column was subtracted from this value to give a net value of viscosity.

DISCUSSION OF EXPERIMENTAL METHOD

It was convenient to present the experimental data in the form of plots of viscosity *vs.* superficial air velocity as functions of such variables as particle size, paddle position, and type of gas distributor. Typical plots are shown in Figures 3 through 7 for single sizes of glass beads. Figure 8 illustrates typical results for mixtures of beads.

Preliminary studies indicated that the paddle size did not affect the shape of the curve of viscosity *vs.* superficial velocity, but only tended to displace the values of viscosity by a constant amount. This viscosity displacement was a function of the volume swept out by the rotating paddle. Studies on both the large and a smaller 2.75-inch column indicated that the angular velocity of the paddle did not severely affect the viscosity *vs.* superficial velocity curves. From studies made at angular velocities of 50, 100, 150, and 200 r.p.m., it was observed that the curves were all of the same shape, but once again were displaced upward on the viscosity scale. On the basis of these preliminary studies it was decided to use a $\frac{3}{4} \times \frac{3}{4} \times \frac{1}{16}$ inch paddle at an angular velocity of 200 r.p.m. for this investigation of viscosity.

Table I. Glass Bead Sizes

Code No.	Average Diameter	
	Inch	Microns
4	0.040	1020
9	0.019	484
10A	0.011	280
13	0.005	127
090	0.011	280
120	0.0045	115
150	0.003	76.5

Because a slight amount of wobbling motion was induced into the extended shaft by the viscometer chuck, it was imperative to ascertain whether this affected the measurements. To accomplish this, a precision ball bearing was attached to the shaft 6 inches below the chuck. The bearing was stabilized and centered by a bracket attached to the positioner. This attachment essentially removed all wobble

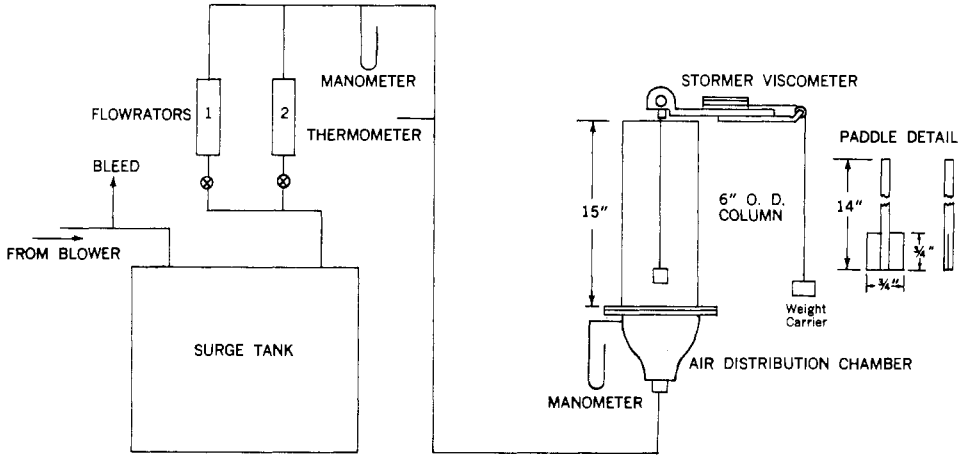

Figure 2. Diagram of experimental apparatus

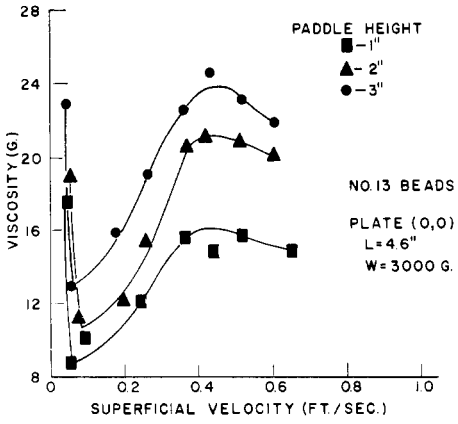

Figure 3. Effect of longitudinal paddle placement with a porous plate air distributor

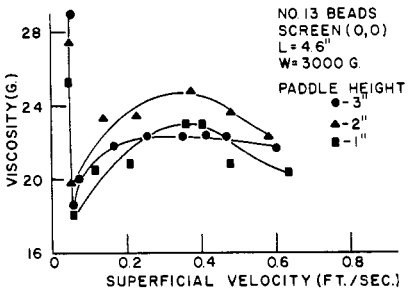

Figure 4. Effect of longitudinal paddle placement with a 200-mesh screen air distributor

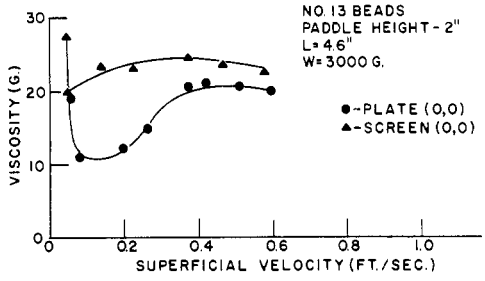

Figure 5. Comparison of screen and porous plate air distributors

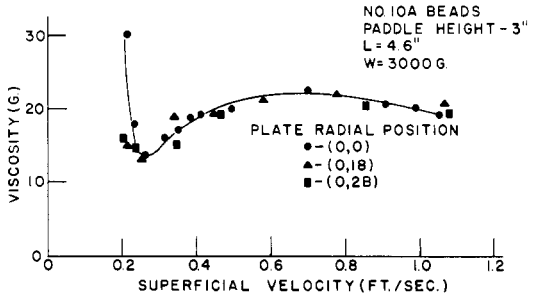

Figure 6. Effect of radial paddle placement with porous plate air distributor

from the extended shaft. Plots of viscosity *vs.* superficial velocity indicated that curves obtained on runs with the bearings were displaced from runs without the bearing by an amount equal to the weight required to overcome the friction of the bearing, thus indicating that the slight wobbling effect induced by the viscometer chuck did not affect the measured viscosity values.

The measured viscosity values were highly reproducible. The precision of measurement with the porous plate distributor was ± 0.2 gram; with the 200-mesh screen distributor, ± 0.3 gram.

DISCUSSION OF RESULTS

The plots of viscosity *vs.* superficial velocity in Figures 3 through 9 all show the same characteristic curve. The viscosity at low gas rates was very high and decreased rapidly with increased air velocity. At intermediate air velocities the viscosity curve began to increase until it passed through a maximum and thereafter it showed a steady decline. The region of low gas velocity showed a rapidly decreasing viscosity due to aeration of the bed. At the intermediate air velocities, the region of retarded bed expansion, the turbulence of the bed was increased in the form of bed turnover, while the density remained approximately constant. This caused the viscosity to increase, because of the greater number of collisions with the paddle. This was the region corresponding to Region II. At higher gas velocities the density began to decrease rapidly and thereby it became the controlling viscosity factor. The viscosity decreased steadily until an equilibrium was attained between the decreasing density effect and the increasing particle velocity effect. This investigation was concerned mostly with Regions I and II, because the size of the apparatus limited the investigations of high gas velocities. Although a few runs reached the equilibrium value, it was assumed from the work of Matheson, Herbst, and Holt (*3*) that each curve had such a value.

Longitudinal profiles using a porous plate air distributor for bead sizes 9, 10A, and 13 (Figure 3) all showed the same trend. The plots of viscosity *vs.* superficial velocity showed an increased viscosity as the paddle was moved away from the fluid distributor. The porous plate gave very small bubbles at the bottom of the bed, which grew as they rose through the bed, but did not exceed an approximate diameter of 1 inch at the surface of the bed. At the bottom of the bed, the large number of small bubbles created a very uniform bed. As the bubbles rose through the column and air further segregated from the particles, the upper stages of the bed became more nonuniform and turbulent. The increased nonuniformity and turbulence caused an increase in viscosity. As the bubble size continues to increase, the bubbles will begin to envelop the paddle completely, causing the paddle's speed to increase rapidly until the particles once again begin to strike the paddle. This effect has a tendency to lower the viscosity measurement. Although this effect was not observed with the No. 9, 10A, or 13 beads, it was observed with the No. 4 beads which, being extremely large compared to the above beads, allowed the bubble size to reach approximately 2 to 2.5 inches at the surface of the bed. In this case the viscosity was highest at approximately the middle of the bed.

The longitudinal profiles obtained using a 200-mesh screen as a distributor (Figure 4) showed that the bed behavior was different from that obtained with a porous plate distributor. The viscosity was low at the bottom of the bed, increased at the center, and decreased again near the top of the bed. This behavior was due to the greater bubble size at the bottom of the bed. The increased bubble size at the distributor caused more bed turbulence and less uniformity in the bed. The surface bubbles, with the screen distributor, were 2 to 3 inches in diameter, causing envelopment of the paddle. Consequently, the viscosity decreased near the top of the bed.

Figure 5 indicates that at similar positions in the bed the screen distributor gave a higher viscosity than the porous plate distributor for the same bead size. This indicates that a screen distributor gave a less uniform and more turbulent bed than a porous plate.

Radial profiles using the porous plate distributor (Figure 6) showed that although differences did occur at some points, in the air velocity range studied, there was no clear-cut difference to be noted in viscosity *vs.* superficial velocity plots taken at different radial positions. Radial viscosity measurements using a screen distributor (Figure 7) showed distinct radial differences. The viscosity was lowest at the center of the column and increased to a maximum at the walls.

The bubbles in a porous plate-distributed bed occurred rather randomly in position, while the bubbles in a screen-

distributed bed seemed to occur mostly at the center of the bed. This caused the particle flow in the screen-distributed bed, as pointed out by Othmer (5), to be up at the center and down at the walls of the bed. The viscosity results confirm the visual observation that the two air distributors gave different types of beds. The porous plate gave a bed which was uniform radially because of the random bubble position, while the screen produced radial uniformity gradients due to the set pattern of particle flow which was produced by the concentration of bubbles at the center of the column. A comparison of screen and plate viscosity plots showed that the screen values were consistently higher than those of the plate, indicating once again that the screen produced a more turbulent and less uniform bed than did the plate distributor.

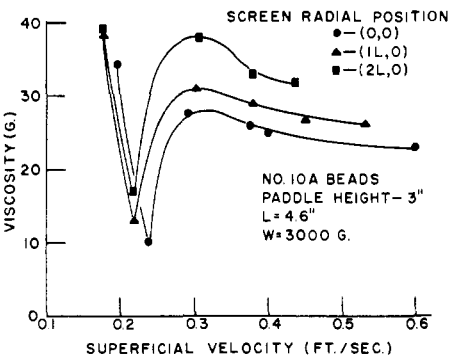

Figure 7. Effect of radial paddle placement with 200-mesh screen air distributor

In the study of blends, the viscosity measurements were made at a paddle height of 3 inches in a bed of $L/D = 1$. The plots of viscosity *vs.* superficial velocity for binary blends (Figure 8) all showed the same characteristic curve that was obtained in single-component studies. Region I of the binary blends was not studied because the blends had a tendency to separate at low gas velocities, because of the comparatively high velocity of the fine component and the

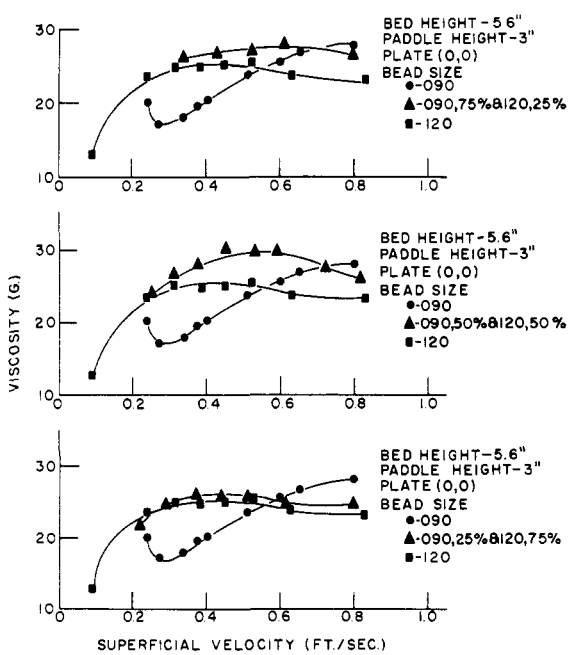

Figure 8. Viscosity vs. flow rate for binary blends

low velocity of the coarse component. Region II, the region most throughly studied, showed the viscosity of blends to be higher than the viscosity of either of the components. This effect was due to the smaller void fraction of the blend (Table II) which concentrated more mass (or particles) in a given volume. This increase in particle concentration in the region of low bed expansion caused an increased viscosity due to the greater number of particles which collided with the paddle per unit time. In Region III where the bed density became a true function of air velocity, the viscosity of the blend followed Kendahl's rule, as was proposed by Furukawa and Ohmae (*1*).

$$\text{Log } \mu_{mix} = y_a \log \mu_a + y_b \log \mu_b$$

In an effort to examine further the existence of Region II on the viscosity *vs.* superficial velocity plot, measurements were made in a column, 2.75 inches in inside diameter. The plots obtained from this apparatus retained the same characteristic curve, and the values obtained by using a screen distributor were once again higher than those obtained when a porous plate was used.

CONCLUSIONS

A study of fluidized beds at low expansion values indicates that a plot of viscosity *vs.* superficial velocity may be divided into three regions. In Region I, the region of low gas rate, the viscosity decreases rapidly with increasing velocity. In Region II, the region of intermediate air velocity, the viscosity tends to increase and pass through a maximum, with increased gas velocity, while in Region III, the region of high gas velocity, the viscosity decreases at a steady rate until an equilibrium value is attained.

A comparison of the results made with the porous plate distributor, and with the 200-mesh screen distributor, shows marked differences in behavior. With the screen, definite radial viscosity variations were noted, which were almost entirely lacking in runs made with the porous plate. The viscosity measurements thus indicated that the uniformity of the fluidized bed in the radial direction was higher in the bed with the porous plate distributor. This conclusion was verified by visual observation. These results suggest that the viscosity measured as described here could serve as a measure for the uniformity of fluidized beds at various points.

A corollary of the above conclusion is that consideration

Table II. Void Fraction of Unaerated Beads

Bead Size Distribution	Void Fraction
No. 090	0.415
No. 120	0.410
No. 150	0.405
No. 090, 75% No. 120, 25%	0.355
No. 090, 50% No. 120, 50%	0.365
No. 090, 25% No. 120, 75%	0.363
No. 090, 75% No. 150, 25%	0.295
No. 090, 50% No. 150, 50%	0.320
No. 090, 25% No. 150, 75%	0.325

Table III. Viscosity Data for Column 5.75 Inches in Inside Diameter

h_p, Inches	h, Inches	Vel., Ft./Sec.	μ, G.
3000 Grams of 10A Beads, Plate, 4.6-Inch Bed			
3.0 (0,0)	4.8	0.268	13.6
	4.7	0.237	18.1
	4.7	0.216	30.6
	5.1	0.319	16.3
	5.3	0.350	17.1
	5.4	0.383	18.6
	5.5	0.41	19.1
	5.8	0.49	20.1
	6.3	0.70	22.6
	6.6	0.91	20.6
	6.9	0.98	20.0
	7.1	1.05	19.1
3.0 (1L,0)	...	0.210	33.6
	...	0.260	12.6
	...	0.337	15.6
	...	0.375	16.6
	...	0.440	17.1
	...	0.560	18.6
	...	0.670	18.7
	...	0.890	19.1
	...	1.02	18.1
	...	1.08	17.9
3.0 (2L,0)	...	0.222	28.1
	...	0.277	13.6
	...	0.325	15.1
	...	0.365	17.1
	...	0.48	19.4
	...	0.64	22.1
	...	0.77	22.1
	...	0.89	23.1
	...	0.99	24.7
	...	1.09	23.6
2.0(0,0)	...	0.222	14.3
	...	0.210	29.1
	...	0.265	11.3
	...	0.320	13.2
	...	0.370	12.1
	...	0.46	15.6
	...	0.65	18.6
	...	0.99	17.9
	...	1.02	17.3
	...	1.20	17.1
1.0 (0,0)	...	0.220	35.9
	...	0.262	9.1
	...	0.302	10.1
	...	0.385	9.7
	...	0.450	9.9
	...	0.660	14.6
	...	0.750	14.6
	...	0.980	14.4
	...	1.20	12.5
2000 Grams of 10A Beads, Plate, 3-Inch Bed			
2.0 (0,0)	3.05	0.220	19.1
	3.10	0.284	10.1
	3.25	0.302	10.9
	3.50	0.365	11.6
	3.70	0.49	13.6
	4.10	0.63	14.7
	4.60	0.80	15.1
	4.90	1.07	14.8
	5.10	1.16	14.3
	5.30	1.28	14.1
1.0 (0,0)	...	0.223	40.9
	...	0.267	12.6
	...	0.310	9.6
	...	0.370	9.4
	...	0.49	9.1
	...	0.59	10.6
	...	0.91	12.1
	...	1.09	12.4
	...	1.25	12.7
	...	1.43	11.5
1000 Grams of 10A Beads, Plate, 1.5-Inch Bed			
0.5 (0,0)	1.50	0.216	18.1
	1.60	0.261	12.1
	1.70	0.313	7.9
	1.80	0.370	6.6
	2.00	0.51	8.4
	2.20	0.71	9.3
	2.50	1.09	8.3
	2.70	1.26	8.0
	2.90	1.55	7.9
3000 Grams of 10A Beads, Plate, 4.6-Inch Bed			
3.0 (0,1B)	...	0.255	13.6
	...	0.216	15.1
	...	0.348	19.1
	...	0.45	19.9
	...	0.58	21.3
	...	0.78	22.1
	...	1.07	20.9
3.0 (0,2B)	...	0.204	16.1
	...	0.240	14.6
	...	0.350	15.1
	...	0.47	19.1
	...	0.87	21.1
	...	1.08	19.9
2.0 (0,1B)	...	0.197	19.1
	...	0.240	14.1
	...	0.347	17.1
	...	0.47	19.1
	...	0.72	20.3
	...	1.02	19.3
2.0 (0,2B)	...	0.220	19.1
	...	0.240	15.9
	...	0.343	16.1
	...	0.50	18.1
2.0 (0,2B)	...	0.72	18.1
	...	1.03	18.2
	...	1.19	19.2
4000 Grams of 13 Beads, Plate, 6.3-Inch Bed			
5.0 (0,0)	6.3	0.057	19.9
	6.5	0.085	10.1
	6.8	0.108	12.1
	6.9	0.131	14.1
	7.1	0.180	16.1
	7.4	0.255	18.6
	8.0	0.365	19.3
	8.3	0.37	19.6
	8.5	0.40	21.3
	9.0	0.47	19.9
3.0 (0,0)	...	0.057	16.1
	...	0.117	10.8
	...	0.174	16.1
	...	0.260	17.6
	...	0.350	19.6
	...	0.40	21.6
	...	0.49	22.4
1.0 (0,0)	...	0.070	13.1
	...	0.160	16.4
	...	0.235	17.2
	...	0.310	17.1
	...	0.365	18.9
	...	0.41	19.6
	...	0.49	20.1
	...	0.053	46.1
3000 Grams of 13 Beads, Plate, 4.6-Inch Bed			
3.0 (0,0)	4.7	0.057	12.9
	5.2	0.177	15.9
	5.5	0.270	19.1
	6.1	0.365	22.6
	6.3	0.44	24.6
	6.8	0.52	23.1
	7.0	0.61	21.9
	4.6	0.051	22.9
3000 Grams of 13 Beads, Plate, 4.6-Inch Bed			
3.0 (1L,0)	...	0.053	21.9
	...	0.057	12.9
	...	0.166	14.6
	...	0.268	17.6
	...	0.365	20.5
	...	0.42	21.1
	...	0.50	21.1
	...	0.65	19.6
	...	0.72	18.4
3.0 (2L,0)	...	0.054	14.1
	...	0.051	20.9
	...	0.169	15.6
	...	0.246	17.3
	...	0.351	23.1
	...	0.43	23.1
	...	0.49	23.6
	...	0.59	23.1
	...	0.65	23.9
	...	0.69	22.9
3.0 (0,1B)	...	0.064	6.4
	...	0.051	17.0
	...	0.178	12.1
	...	0.361	20.1
3.0 (0,2B)	...	0.090	11.1
	...	0.058	9.1
	...	0.051	18.3
	...	0.216	15.1
	...	0.354	17.4
2.0 (0,0)	...	0.059	19.0
	...	0.080	11.1
	...	0.200	12.1
	...	0.260	15.3
	...	0.370	20.6
	...	0.420	21.1
	...	0.510	20.9
	...	0.600	20.1
1.0 (0,0)	...	0.059	8.9
	...	0.096	10.1
	...	0.246	12.1
	...	0.368	15.6
	...	0.440	14.9
	...	0.520	15.6
	...	0.650	14.4
	...	0.051	17.6
2000 Grams of 13 Beads, Plate, 3.1-Inch Bed			
2.0 (0,0)	3.25	0.053	29.1
	3.4	0.090	6.6
	3.5	0.184	10.1
	3.7	0.264	12.6
	3.8	0.350	13.8
	4.3	0.38	16.1
	4.5	0.48	17.6
	4.6	0.57	17.1
	4.8	0.64	15.5
	5.3	0.76	13.2
	6.0	1.07	12.1
	7.2	1.47	11.4
	6.8	1.25	11.7
1.0 (0,0)	...	0.050	19.1
	...	0.093	9.1
	...	0.225	9.1
		0.298	9.6
	...	0.370	13.6
	...	0.42	12.6
	...	0.56	13.1
	...	0.64	12.1
	...	0.84	11.4
1000 Grams of 13 Beads, Plate, 1.60-Inch Bed			
0.5 (0,0)	1.6	0.060	7.1
	1.6	0.051	7.4
	1.8	0.185	7.9
	2.2	0.290	8.1

Table III. Continued

h_p, Inches	h, Inches	Vel., Ft./Sec.	μ, G.
1000 Grams of 13 Beads, Plate, 1.60-Inch Bed			
0.5 (0,0)	2.3	0.368	10.6
	2.4	0.40	10.0
	2.5	0.53	9.6
	2.8	0.67	8.7
3000 Grams of 10A Beads, Screen, 4.6-Inch Bed			
3.0 (0,0)	4.7	0.296	28.0
	4.9	0.376	26.1
	4.6	0.238	10.1
	4.6	0.196	34.4
	5.0	0.40	24.9
	5.4	0.70	23.0
	5.5	0.93	22.8
3.0 (1L,0)	...	0.180	38.4
	...	0.216	13.1
	...	0.303	31.1
	...	0.371	29.1
	...	0.45	26.9
	...	0.53	26.7
3.0 (2L,0)	...	0.179	39.4
	...	0.218	17.1
	...	0.307	38.4
	...	0.380	33.4
	...	0.44	31.9
	...	0.54	31.4
2.0 (0,0)	...	0.180	59.4
	...	0.200	27.1
	...	0.218	8.1
	...	0.297	32.0
	...	0.370	30.2
	...	0.41	30.9
	...	0.52	29.9
1.0 (0,0)	...	0.170	48.4
	...	0.218	28.1
	...	0.295	31.2
	...	0.374	33.2
	...	0.42	31.6
	...	0.52	28.0
	...	0.75	11.5
	...	0.220	27.7

h_p, Inches	h, Inches	Vel. Ft./Sec.	μ, G.
2000 Grams of 10A Beads, Screen, 3.1-Inch Bed			
1.0 (0,0)	3.1	0.170	34.4
	3.1	0.207	28.1
	3.2	0.281	30.1
	3.4	0.375	25.1
	3.6	0.50	24.9
	3.8	0.59	23.7
2.0 (0,0)	...	0.192	27.1
	...	0.170	47.4
	...	0.200	21.2
	...	0.371	20.6
	...	0.47	19.2
	...	0.59	18.1
3000 Grams of 13 Beads, Screen, 4.6-Inch Bed			
3.0 (0,0)	4.7	0.051	18.6
	4.8	0.066	20.1
	5.0	0.163	21.9
	5.3	0.257	22.4
	6.0	0.350	22.4
	6.3	0.41	22.4
	6.5	0.47	22.5
	4.6	0.050	29.1
	6.7	0.60	21.8
3.0 (1L,0)	...	0.051	21.1
	...	0.070	24.1
	...	0.177	24.3
	...	0.280	23.2
	...	0.370	25.1
	...	0.40	25.1
	...	0.48	24.0
3.0 (2L,0)	...	0.052	32.6
	...	0.076	24.1
	...	0.178	27.4
	...	0.280	29.0
	...	0.360	30.2
	...	0.39	31.0
	...	0.49	29.0

h_p, Inches	h, Inches	Vel., Ft./Sec.	μ, G.
3000 Grams of 13 Beads, Screen, 4.6-Inch Bed			
2.0 (0,0)	...	0.056	19.9
	...	0.140	23.4
	...	0.230	23.4
	...	0.375	24.9
	...	0.050	27.4
	...	0.47	23.7
	...	0.58	22.6
1.0 (0,0)	...	0.057	18.1
	...	0.110	20.6
	...	0.205	20.9
	...	0.360	23.1
	...	0.050	25.2
	...	0.40	23.1
	...	0.48	20.9
	...	0.64	20.3
2000 Grams of 13 Beads, Screen, 3.1-Inch Bed			
1.0 (0,0)	...	0.056	19.1
	...	0.140	15.4
	...	0.233	15.9
	...	0.365	16.0
	...	0.43	16.1
	...	0.56	16.5
	...	0.068	18.0
2.0 (0,0)	3.1	0.056	14.9
	3.1	0.078	14.7
	3.3	0.200	14.1
	3.4	0.276	14.0
	3.6	0.366	16.0
	4.0	0.48	16.2
	4.2	0.54	15.1
3435 Grams of 090 Beads, Plate, 5.6-Inch Bed			
3.0 (0,0)	...	0.337	18.1
	...	0.375	19.9
	...	0.40	20.5
	...	0.51	24.1
	...	0.60	25.8
	...	0.65	27.1
	...	0.81	28.2
	...	0.271	17.1
	...	0.231	20.2
3435 Grams of 120 Beads, Plate, 5.6-Inch Bed			
3.0 (0,0)	...	0.090	13.1
	...	0.246	23.9

should be given to the type of distributor used in experimental work on fluidized beds. These results indicate that the distributor may markedly influence the behavior of the bed, exclusive of all other variables.

Table III gives viscosity data for a column 5.75 inches in inside diameter. Complete results are included in Haas's thesis (2).

ACKNOWLEDGMENT

The authors thank the Oak Ridge Institute of Nuclear Studies for the fellowship grant to F.C. Haas.

NOMENCLATURE

(0,0) = Center
(1L,0) = 1 inch left of center on horizontal left-right axis
(2L,0) = 2 inches left of center on horizontal left-right axis
(0,1B) = 1 inch back of center on horizontal front-back axis
(0,2B) = 2 inches back of center on horizontal front-back axis
a = component a
b = component b
D = column diameter, inches
h = bed height, inches
h_p = paddle height, distance from paddle to distributor, inches
L = height of unaerated bed, inches
W = weight of beads in bed, grams
y = volume fraction
μ = viscosity of a fluidized bed, grams

LITERATURE CITED

(1) Furukawa, J., Ohmae, T., *Ind. Eng. Chem.* **50**, 822 (1958).
(2) Haas, F.C., M.S. thesis, Rensselaer Polytechnic Institute, Troy, N. Y., 1958.
(3) Kramers, H., *Chem. Eng. Sci.* **1**, *No. 1*, 35 (1952).
(4) Matheson, G.L., Herbst, W.A., Holt, P.H., *Ind. Eng. Chem.* **41**, 1094 (1949).
(5) Othmer, D.F., "Fluidization," pp. 14–15, Reinhold, New York, 1956.

RECEIVED for review August 17, 1959. Accepted March 31, 1960.